ORIGINAL PAPER

Synthesis and Evaluation of Mesoporous Silica Nanoparticle Catalyst Supports Prepared from South African Coal Fly Ash

Mathibela E. Aphane[1,2] · Emile D. Maggott[3] · Frédéric J. Doucet[4] · Selwyn F. Mapolie[3] · Marilé Landman[1] · Elizabet M. van der Merwe[1]

Abstract

The development of environmentally sustainable catalytic reaction systems for the oxidation of organic compounds has gained significant interest, with widespread application across various industries. This study investigates the suitability of mesoporous silica nanoparticles, synthesized from coal fly ash, as catalyst supports in the oxidation of veratryl alcohol, a compound that serves as a model to mimic the oxidation behavior of lignin-derived structures commonly found in biomass waste. A Cu(II) salicylaldimine complex was employed as the catalyst, with *tert*-Butyl hydrogen peroxide as the oxidant. Silica catalyst supports were synthesized from coal fly ash derived Na_2SiO_3 solutions. The effect of pre-dealumination of coal fly ash during Na_2SiO_3 preparation, variation of the surfactant in silica nanoparticle synthesis, and storage conditions of the catalyst supports on the performance of the coal fly ash derived silica catalyst supports were evaluated and compared to the performance of MCM-41 and SBA-15. The textural properties of the coal fly ash derived silica catalyst supports were notably influenced by the choice of surfactant used during its synthesis, while storage conditions affected the abundance of silanol groups necessary for successful catalyst immobilisation.

Graphical Abstract
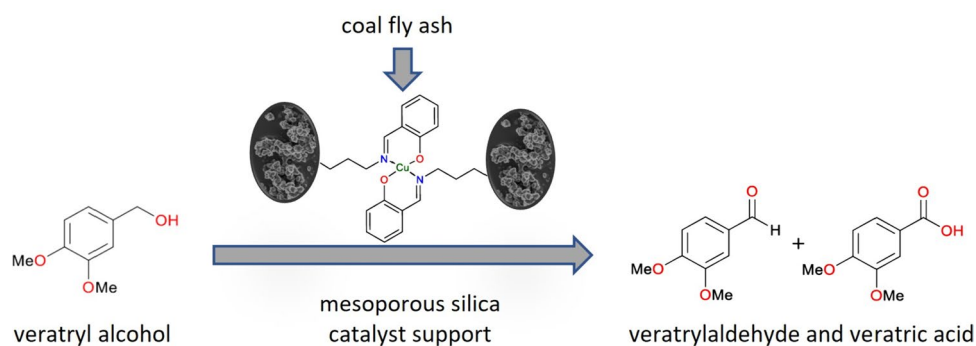
✉ Elizabet M. van der Merwe
   liezel.vandermerwe@up.ac.za

[1] Chemistry Department, University of Pretoria, Lynnwood Road, Pretoria 0001, South Africa

[2] Department of Chemistry, UNISA, PO Box 392, Pretoria 0003, South Africa

[3] Department of Chemistry, Stellenbosch University, Stellenbosch, South Africa

[4] Council for Geoscience, 280 Pretoria Road, Private Bag X112, Pretoria 0001, South Africa

Highlights

- High-purity SiO_2 nanoparticle catalyst supports were produced from coal fly ash
- Fly ash derived catalyst supports can be applied in heterogeneous catalysis

- The surfactant used during nano-SiO$_2$ synthesis influenced its textural properties
- The abundance of silanol groups affected the efficiency of catalyst immobilization

Statement of Novelty

We previously demonstrated the synthesis of amorphous mesoporous silica nanoparticles from sodium silicate solutions which were prepared from a South African classified coal fly ash. In this paper, we assess the performance of these silica nanoparticles as heterogeneous catalyst supports and compare their performance to that of MCM-41 and SBA-15 in the oxidation of veratryl alcohol, using a Cu(II) salicylaldimine complex as catalyst. We report on the effect of pre-dealumination of coal fly ash during Na$_2$SiO$_3$ preparation, the influence of silica nanoparticle storage conditions, and the effects of varying the surfactant during silica nanoparticle synthesis, on the performance of the coal fly ash derived catalyst supports. The utilization of these catalyst systems could significantly contribute to the development of cost-effective and sustainable processes for producing value-added products from coal combustion residues and biomass.

Introduction

The design of environmentally friendly catalytic systems for the oxidation of organic compounds has gained significant interest and is being increasingly applied in various industries. Studied processes include the oxidation of hydrocarbons like ethylbenzene, cyclohexene, benzyl alcohol, styrene and veratryl alcohol, to produce valuable oxygenates such as acetophenone, benzaldehyde, benzoic acid, aldehydes, ketones and veratrylaldehyde [1–6]. Studies related to the oxidation of lignin, a major component of biomass waste, are essential for developing sustainable and environmentally friendly processes in industries such as biorefining, the production of biofuel and renewable materials (e.g., bioplastics), and the management of lignin-rich waste streams [7]. Veratryl alcohol (3,4-dimethoxy benzyl alcohol) is often used as model compound in laboratory studies to mimic the oxidation behaviour of lignin-derived structures [8–10]. Various catalytic systems have been studied in the literature for accelerating the oxidation of veratryl alcohol into veratrylaldehyde and/or veratric acid. [1, 3, 8–12]. Selectivity towards the formation of veratrylaldehyde is generally preferred due to its application in the food and fragrance industries [1, 10]. Many of the catalytic systems applied in the oxidation of veratryl alcohol have shown improved catalytic activity and selectivity through immobilization of the

catalyst on an inorganic support material, thereby creating a heterogeneous catalyst.

The published literature consistently highlights the advantages of catalyst immobilization to include the enhancement of catalyst stability under various reaction conditions, leading to improved reusability over successive catalytic cycles as well as the facilitation of simple separation of the catalytic system from the reaction mixture, resulting in products of higher purity [13, 14]. Ordered mesoporous silica is widely recognized for its excellent performance as a catalyst support and is one of the most extensively used metal oxides in heterogeneous catalysis, primarily due to its favourable combination of textural properties (i.e., uniform pore sizes in the mesopore range (2–50 nm), high surface areas (~ 1000 m^2 g), and large pore volumes (~ 1 cm^3 g)) [15–17]. Their small particle sizes, high thermal and chemical resistance, along with excellent sorption properties arising from their large surface area and porous structure, make them highly suitable as catalyst supports. Among these, MCM-41 [18], MCM-48 [18], SBA-15 [19], and MCFs [20] have undergone extensive study for catalyst immobilization. Some of these mesoporous silica materials (e.g., MCM-41 and SBA-15) are commercially available.

Jana et al. [21] reported the immobilization of Cu(II) salicylaldimine complexes on MCM-41 as catalyst for the oxidation of cyclohexene, using *tert*-Butyl hydrogen peroxide (TBHP) as an oxidant, resulting in good selectivity and yields. In a study by Malumbazo and Mapolie [22], Cu(II) and Co(II) salicylaldimine complexes were immobilized on MCM-41, SBA-15 and Davisil 710 and tested as catalysts for cyclohexene oxidation, utilizing hydrogen peroxide as the oxidant under an oxygen atmosphere. Their research investigated the impact of substituents on the salicylaldimine ring and the nature of the silica support on catalytic activity. The results highlighted the significant role played by the nature and physical properties of the catalyst support in the selectivity of the reaction system. Kotzé and Mapolie [23] investigated the performance of Ru(II) complexes supported on MCM-41 and SBA-15 as catalyst precursors for the selective oxidative cleavage of 1-octene. The immobilized heterogeneous catalysts exhibited superior activity compared to their homogeneous counterparts and demonstrated control over the selective formation of aldehydes or carboxylic acids. The results obtained in the studies by Malumbazo [22] and Kotzé [23] stimulated our interest in the application of amorphous mesoporous silica nanoparticles produced from coal fly ash (CFA) as alternative catalyst support to the commercially available MCM-41 and SBA-15.

CFA is a by-product from the combustion of pulverised coal in thermoelectric power stations. In South Africa, only about 7% of the ca. 35 million tons of CFA produced annually is recycled, mainly in the cement and construction industry [24]. Given its high silicon (Si) and aluminium

(Al) content, CFA holds potential as a valuable secondary resource of purified silica and alumina. In our previous research, we successfully demonstrated the synthesis of amorphous mesoporous silica nanoparticles from Na_2SiO_3 solutions derived from a South African CFA sample [25]. We evaluated two methods for preparing Na_2SiO_3 from CFA, with the aim to determine whether pre-treatment to remove the reactive aluminium from CFA is beneficial to silica nanoparticles synthesis. These Na_2SiO_3 solutions were then employed as silica precursors in the synthesis of silica nanoparticles using a sol–gel method, resulting in silica nanoparticles with purities ranging between 98.8 and 99.3%.

In this paper, we assess the suitability and performance of the CFA-derived amorphous mesoporous silica nanoparticles as heterogenous catalyst supports and compare their performance to that of MCM-41 and SBA-15 in the oxidation of veratryl alcohol, using a Cu(II) salicylaldimine complex as catalyst. Specific objectives were to

(i) Determine whether pre-dealumination of the CFA during Na_2SiO_3 preparation influences the performance of the CFA-derived catalyst support.
(ii) Investigate the effect of varying the surfactant on the physical properties of CFA-derived catalyst supports.
(iii) Study the influence of storage conditions on the performance of the CFA-derived catalyst supports.
(iv) Examine the effects of varying the surfactant during silica nanoparticle synthesis on the performance of the CFA-derived silica catalyst supports.

To our knowledge, the application of CFA-derived silica nanoparticles as catalyst supports has not been reported before.

Experimental

Materials

A representative sample of a classified, ultrafine siliceous CFA sample was obtained from Ash Resources (Pty) Ltd. This commercial-grade CFA is air-classified on site and is specified to have a mean particle size between 3.9 and 5.0 μm, with more than 90% of the volume distribution of its particles having a diameter smaller than 11 μm. The CFA sample was sub-divided using a rotary splitter to obtain representative homogeneous sub-samples.

Deionised water (analytical grade, electrical conductivity < 1 μS cm^{-1}) was used for all experiments. H_2SO_4 (analytical grade, 98% w/w), polyethylene glycol (PEG, 6000), barium chloride (analytical grade), sodium lauryl sulphate (SLS, analytical grade) and cetyl pyridinium chloride (CPC, analytical grade) were obtained from Merck, South Africa.

The NaOH solution (analytical grade, 50.0% w/w) and n-butanol (analytical grade) were obtained from Radchem, South Africa. Cetyl-trimethyl bromide (CTAB, analytical grade) was obtained from Minema, South Africa. Acetonitrile, toluene, dichloromethane, methanol, veratryl alcohol and *tert*-Butyl hydrogen peroxide (TBHP) were obtained from Sigma-Aldrich. Toluene and DCM were purified using a Pure Solv™ micro solvent purifier fitted with activated alumina columns. Methanol, acetone and ethanol were purified by distillation over magnesium filings and iodine. Acetonitrile was purified by distillation over phosphorous pentoxide.

Preparation of CFA-Derived Sodium Silicate Solutions (S_{alk-sq} and S_{alk-d})

CFA was subjected to two distinct leaching processes in order to prepare Na_2SiO_3 solutions of different grades (Fig. 1). Process 1 was a two-stage sequential acid-alkaline leaching process (SAAL) which involved (i) a H_2SO_4 leaching step for the preferential extraction of Al over Si, followed by (ii) the preferential extraction of Si over Al from the resulting residues using NaOH. Process 2 was a direct alkaline leaching (DAL) process, which consisted of a single-stage elemental extraction from CFA using NaOH, *i.e.* without the preceding acid leaching step used in SAAL. These leaching procedures and subsequent characterisation of the sodium silicate solutions were detailed earlier [25].

Preparation of Silica Catalyst Supports (Si_{SAAL}, Si_{DAL}, Si_{CTAB}, Si_{CPC}, Si_{SLS}, Si_{PEG}, MCM-41 and SBA-15)

Silica catalyst supports were prepared from the CFA-derived sodium silicate solutions via a sol–gel method as previously described [25]. 20 ml of a 3% w/w surfactant solution was sonicated in a 20 Hz ultrasonic water bath at 55 °C for 30 min. 80 ml of sodium silicate solution, equilibrated at 55 °C, was slowly added to the surfactant solution in the ultrasound bath while monitoring the pH of the solution. To initiate the hydrolysis-condensation reaction, 0.5 M H_2SO_4 was gradually added to the sodium silicate solution until a pH of 4 was reached; sonication was continued for another 30 min. The resulting gel mixture was aged overnight at 55 °C in a laboratory oven after which the wet gel silica slurry was separated from the mother liquor by centrifugation. The gel was thoroughly washed with deionised water to remove any remaining Na^+ and SO_4^{2-} ions. Several successive washing cycles were performed to ensure the removal of SO_4^{2-} ions while using $BaCl_2$ to test for the presence of SO_4^{2-} ions in the washing water. This was followed by centrifugation and vacuum-filtration. The resulting filtration cake was distilled using 100 ml n-butanol for 2 h, followed by overnight drying at 120 °C. The resultant powders were subsequently calcined

Fig. 1 Process flow diagrams for the preparation of silica catalyst supports from CFA derived sodium silicate solutions
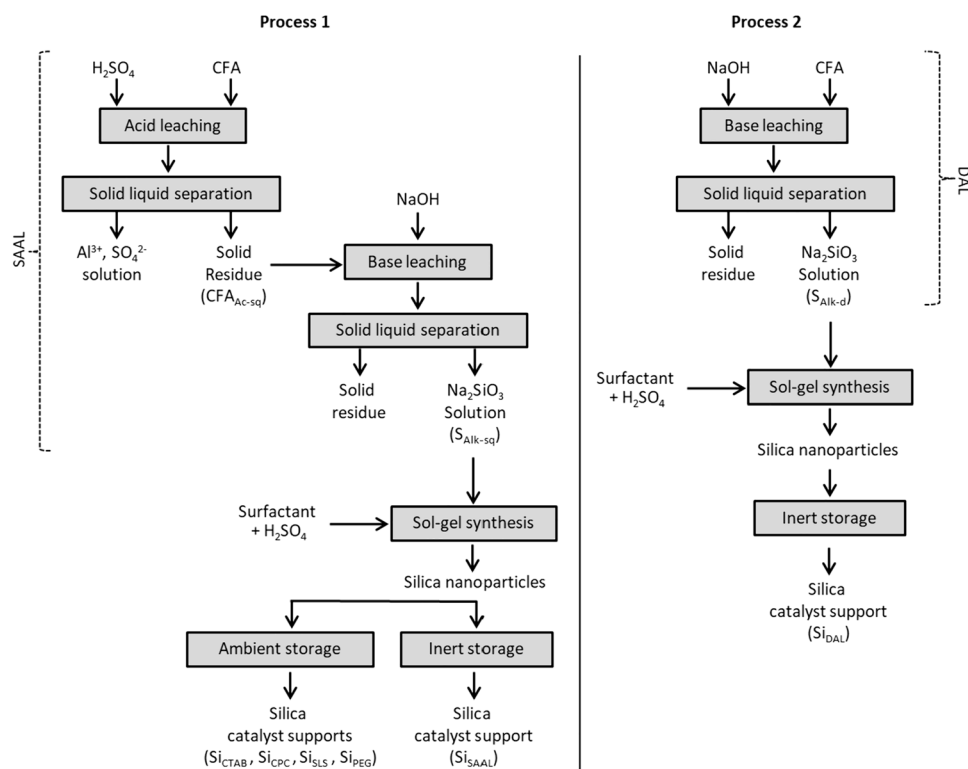
in a laboratory furnace at 650 °C for 2 h (SLS and PEG) or 3 h (CTAB and CPC) to remove the remaining surfactant and n-butanol. When silica samples prepared from CTAB and CPC were heat-treated at 650 °C for 2 h, a greyish coloured powder was obtained, indicating that small traces of surfactant were remaining in the product. By extending the heat treatment at 650 °C to 3 h, a pure white coloured powder was obtained.

The effect of pre-dealumination of CFA during the preparation of sodium silicate solutions was assessed by comparing the properties of the silica catalyst supports synthesized from S_{alk-sq} and S_{alk-d}, which were derived from the SAAL and DAL processes, respectively (Fig. 1). This analysis was carried out using only PEG as the surfactant. The resultant silica powders were stored under inert conditions until their application as catalyst supports. These solid products were labelled Si_{SAAL} and Si_{DAL} respectively.

To investigate the effect of varying the surfactant on the properties of silica catalyst supports obtained from CFA, the above synthesis method was repeated using different surfactants (CTAB, CPC, SLS and PEG) from the Na_2SiO_3 solution prepared via the SAAL method (S_{alk-sq}). This Na_2SiO_3 solution was selected since it resulted in the formation of silica nanoparticles of higher purity [25]. The resultant silica powders were stored under ambient conditions until their application as catalyst supports. The solid products were labelled Si_{CTAB}, Si_{CPC}, Si_{SLS} and Si_{PEG}, respectively.

MCM-41 [26] and SBA-15 [19] were synthesized according to previously reported procedures.

Synthesis of Functionalized 2-(3-Triethoxysilanepropyliminomethyl)-Phenol Ligand

Synthesis and characterisation of the functionalized 2-(3-triethoxysilanepropyliminomethyl)-phenol ligand was reported before [22, 27, 28]. All procedures were carried out under inert conditions using dry nitrogen and utilization of standard Schlenk techniques. Salicylaldehyde (5 mmol, 0.611 g) and 3-aminopropyl-triethoxysilane (5 mmol, 1.10 g) were dissolved in dry THF (6 ml) in a 10 ml microwave reactor tube. A small amount of $MgSO_4$ was added to the tube. This was allowed to react in a microwave reactor for 10 min under a nitrogen atmosphere at 100 W while maintaining a constant temperature of 80 °C. After the allotted time, a bright yellow solution was obtained and filtered to remove the $MgSO_4$. The solvent was removed under reduced pressure and a yellow oil was obtained (1.66 g, 78%). Characterization was achieved by ^{1}H NMR and FT-IR (ATR) spectroscopy.

Characterisation of functionalized ligand: Yellow oil, yield 78%. FT-IR, v/cm^{-1}: 1631 (Imine, HC=N), 1077 (Si–O), 755 (Si–O). ^{1}H NMR (400 MHz, (CDCl$_3$)): δ (ppm) = 13.97 (H_{Ar-OH},s, 1H), 8.67 (H_{imine}, s, 1H), 7.66–7.61 (H_{Ar-H}, m, 1H), 7.58 (H_{Ar-H}, dd, 1H,$^3J_{H-H}$=7.6

Hz, $^4J_{H\text{-}H}$ = 1.7 Hz), 7.29 (H$_{Ar\text{-}H}$, d, 1H, $^3J_{H\text{-}H}$ = 8.3 Hz), 7.20 (H$_{Ar\text{-}H}$, td, 1H, $^3J_{H\text{-}H}$ = 7.6 Hz, $^4J_{H\text{-}H}$ = 1.1 Hz), 3.93 (propyl N-CH$_2$, td, 2H, $^3J_{H\text{-}H}$ = 6.8 Hz, $^4J_{H\text{-}H}$ = 1.1 Hz), 2.21–2.12 (propyl CH$_2$-CH$_2$-CH$_3$-Si, m, $^3J_{H\text{-}H}$ = 8 Hz, 2H), 1.05–1.01 (propyl CH$_2$-CH$_2$-CH$_2$-Si, m, 2H), 4.17 (Si–O–CH$_2$-CH$_3$, q, 6H, $^3J_{H\text{-}H}$ = 7.0 Hz), 1.57 (Si–O–CH$_2$-CH$_3$, t, 9H, $^3J_{H\text{-}H}$ = 7.0 Hz).

Synthesis of Functionalized 2-(3-Triethoxysilanepropyliminomethyl)-Phenolato Cu (II) Complex

The 2-(3-triethoxysilanepropyliminomethyl)-phenol ligand (1.00 mmol, 0.326 g) was dissolved in dry ethanol (5 ml), which resulted in a yellow solution. Cu(OAc)$_2$H$_2$O (0.501 mmol, 0.100 g) was added to the solution containing the ligand, which resulted in a green reaction mixture. The reaction mixture was stirred for 3 h under nitrogen at 80 °C. The solvent was removed *in vacuo* and a green crude powder was obtained. The green crude product was purified by redissolving it in dry dichloromethane (5 ml) after which it was syringe filtered. The solvent was removed from the filtrate in vacuo and a green powder was obtained (0.211 g, 60%).

Characterisation of functionalized Cu(II) complex: Green solid, yield 60%. FT-IR, υ/cm^{-1}: 1620 (C=N), 1047 (Si–O), 755 (Si–O). Elemental Analysis (%): Calc. For C$_{32}$H$_{52}$N$_2$O$_8$Si$_2$ Cu· (712.48 g/mol): C, 53.29; H, 7.36; N, 3.93; Found: C, 53.71; H, 6.99; N, 3.91. Melting Point: 236–239 °C.

Preparation of Immobilized Catalysts (Cu$_{SAAL}$, Cu$_{DAL}$, Cu$_{CTAB}$, Cu$_{CPC}$, Cu$_{SLS}$, Cu$_{PEG}$, Cu$_{MCM-41}$, and Cu$_{SBA-15}$)

The general reaction scheme for preparation of the immobilized catalysts is shown in Fig. 2. Silica powder (1.00 g Si$_{SAAL}$, Si$_{DAL}$ Si$_{CTAB}$, Si$_{CPC}$, Si$_{SLS}$, Si$_{PEG}$, MCM-41 or SBA-15) was suspended in dry toluene (10 ml), which resulted in a white slurry. To this solution, 0.1 g of functionalized complex was added which then resulted in a green reaction mixture. This reaction mixture was stirred at 110 °C for 24 h. After the allotted time, the green reaction mixture was left to cool to room temperature. The mixture was then filtered and washed consecutively with dry methanol (5 × 15 ml). The solid was dried *in vacuo* at 60 °C for 5 h and a light green powder was obtained. The products were labelled Cu$_{SAAL}$, Cu$_{DAL}$, Cu$_{CTAB}$, Cu$_{CPC}$, Cu$_{SLS}$, Cu$_{PEG}$, Cu$_{MCM-41}$, and Cu$_{SBA-15}$, respectively.

Oxidation of Veratryl Alcohol

Veratryl alcohol (0.168 g, 1.0 mmol) was dissolved in dry acetonitrile (10 ml) using a parallel reactor tube. The immobilized catalyst (8.13 mg, 0.025 mmol, 2.0 mol %) was added to the solution and sodium hydroxide (0.2 mmol, 2 M, 100 µl) was added to the tube. *tert*-Butyl hydrogen peroxide was added using appropriate ratios (substrate:oxidant). Addition of TBHP resulted in a white precipitate forming. The reaction mixture was stirred at 25 °C for 6 h and a green reaction mixture was observed. After the allotted time, the reaction reactor tube was quenched in ice-cold water followed by the addition of a small amount of MgSO$_4$. Thereafter, the mixture was filtered, and quantitative analysis of the filtrate was performed using gas chromatography (GC-FID) using *p*-Xylene as internal standard. The general reaction scheme for oxidation of veratryl alcohol is indicated in Fig. 3.

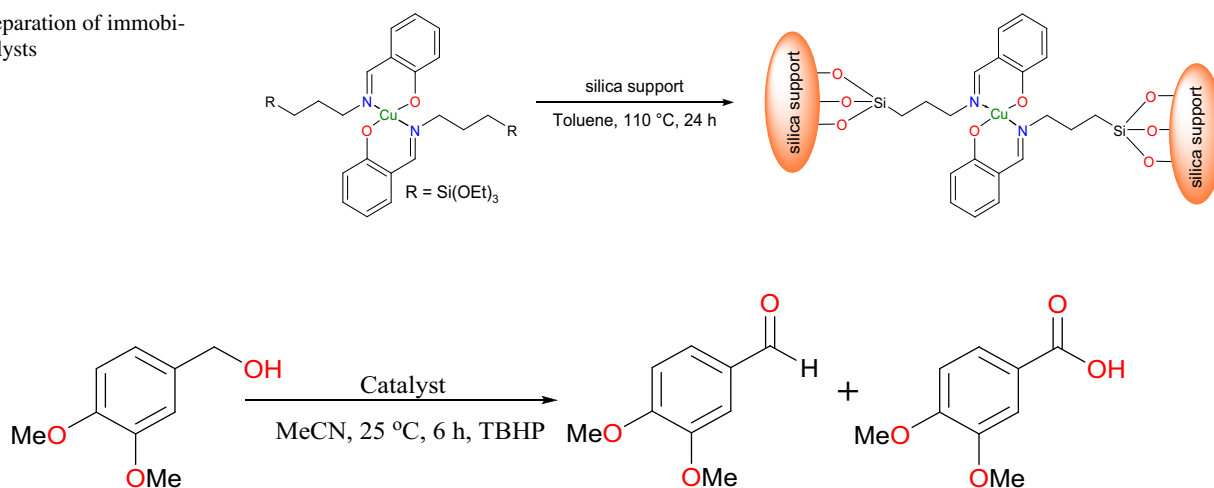**Fig. 2** Preparation of immobilized catalysts

Fig. 3 Reaction scheme for the oxidation of veratryl alcohol to veratrylaldehyde and veratric acid

Recycling Experiments

Recycling of the catalysts was performed after each of the catalytic runs. This entailed subjecting the reaction mixture to centrifugation to isolate the catalysts. The supernatant was decanted leaving the green catalyst material. 5 ml of dry methanol was used to wash the solid to remove any residual product that remained after the centrifuge process. The catalyst suspension in methanol was once again centrifuged at 6000 rpm for an additional 10 min. The resulting supernatant was discarded, and the solid green residue catalyst was dried *in vacuo* for 6 h and then reused in the next catalytic run. The catalysts were recycled for five subsequent runs.

Sample Characterisation Techniques

Detailed descriptions of the sample characterisation techniques applied in this study were reported previously [25, 29]. The elemental composition of the CFA sample was determined by XRF fused bead analysis using an ARL9400XP + XRF spectrometer, Thermo ARL, Switzerland. A glass disk was prepared by fusing a mixture of 1 g CFA with 6 g of $Li_2B_4O_7$ at 1000 °C. The silica catalyst supports were prepared as pressed powders prior to XRF analysis. The mineralogy of CFA and the silica catalyst supports was determined using XRD. XRD patterns were collected from on a PANalyticalX'Pert Pro powder diffractometer with X'Celerator detector and variable divergence and fixed receiving slits with Fe filtered Co-Kα radiation, operated at 40 kV. The phases were identified using X'PertHighscore plus software. The relative phase amounts were estimated using the Rietveld method (Autoquan Program). Twenty percent silicon (Aldrich 99% pure) was also added to each sample for the determination of amorphous content. The samples were micronized in a McCrone micronizing mill and prepared for XRD analysis using a back loading preparation method.

A Zeiss Ultra SS (Germany) FESEM, operated at an acceleration voltage of 1 kV, was used under dry high-vacuum condition to observe the morphology of the silica catalyst supports. The powder was mounted on a double-sided carbon tape by dipping carbon stubs into the samples. Excess material was removed by gentle blowing with compressed nitrogen. The sample was sputter-coated with carbon in an Emitech K550X (Ashford, England). A JEOL JEM 2100F TEM was used to study the topography of the silica catalyst supports. The samples were first dispersed in 100% ethanol with the aid of sonication. A drop of the diluted suspension was poured onto a copper grid, which was then placed into the sample injection holder for analysis.

A TriStar II surface area and porosity analyser (Micromeritics, USA) was used with nitrogen gas as adsorbent to determine the bulk surface area by the Brunauer-Emmet-Teller (BET) theory. The samples were degassed at 300 °C for 3 h before performing the gas adsorption tests.

Catalytic reactions were conducted using a Radleys 12-stage carrousel parallel reactor equipped with an oxygen gas distribution system (Online Resource 1, Fig. S1). Quantitative and qualitative analysis were performed on a Varian 3900 gas chromatograph containing a Cyclosil-β column (30 m × 0.25 mm × 0.25 μm) equipped with a flame ionisation detector (GC-FID), using p-xylene as internal standard.

Results and Discussions

Characterization of Untreated CFA and Composition of CFA-Derived Sodium Silicate Solutions

The chemical compositions of CFA and the CFA-derived sodium silicate solutions (S_{alk-sq} and S_{alk-d}) obtained from the two extraction processes (SAAL and DAL) were reported in detail previously [25]. The CFA sample contained mainly SiO_2 (51.5), Al_2O_3 (33.6), CaO (5.2), Fe_2O_3 (3.4), TiO_2 (1.9), MgO (1.0) and K_2O (1.0%); all reported as mass percentages. Its mineralogy consisted of an amorphous alumina silica glass phase (64.2% m/m) and two crystalline phases, mullite (28.5% m/m) and quartz (7.2% m/m).

The two CFA-derived sodium silicate solutions exhibited similar Si (10.3 g/L) and Na (188 g/L) content, but their Al content differed greatly [25]. Incorporation of a dealumination step, accomplished through acid pre-leaching during the SAAL process, yielded a sodium silicate solution with significantly lower Al content (< 0.2 g/L for S_{alk-sq} *vs* 1.2 g/L for S_{alk-d}). Both solutions contained similar amounts of Fe (± 0.2 g/L) and K (± 0.8 g/L) as impurities. The concentration of P was below 0.1 g/L in both solutions, that of Ca, V and Li were below 0.05 g/L, and the remaining elements occurred in quantities less than 1×10^{-3} g/L. The pH of both Na_2SiO_3 solutions was identical at 11.8.

Characterisation of CFA-Derived Silica Catalyst Supports

Detailed chemical, mineralogical and physical characterisation of Si_{SAAL} and Si_{DAL} obtained via the sol–gel method using PEG as surfactant was published in our previous paper [25]. Both products were characterised by a high level of purity (96.3–98.6% SiO_2 mm^{-1}), with most of the deviation from 100% being due to moisture as a result of the hygroscopic nature of the samples. The product obtained from the DAL process contained a marginally greater amount (% m/m) of Al_2O_3 (0.45%) than that from SAAL (0.13). The CaO (0.2–0.3), MgO (0.1–0.2) and Na_2O (< 0.1%) content of the two products were similar. Minor amounts (< 0.03%) of Fe_2O_3, TiO_2, K_2O, P_2O_5 and SO_3 were observed. Conversion

of the XRF data to a dry mass basis indicated that the actual purity of Si_{SAAL} and Si_{DAL} ranged between 98.8 and 99.3% m/m.

Results obtained for the chemical characterisation of Si_{CTAB}, Si_{CPC}, Si_{SLS} and Si_{PEG} were similar to that of Si_{SAAL}. The actual purities of these samples were 99.3 for Si_{PEG} and > 99.9% for Si_{CTAB}, Si_{CPC} and Si_{SLS}, indicating that the preparation of ultra-pure silica catalyst supports was achieved using the sodium silicate solution prepared by the SAAL process and either CTAB, CPC or SLS as surfactant. These products contained a minor amount of Al_2O_3 (< 0.1 wt. %) and trace amounts of other impurities. The presence of a broad band centred at $2\theta = 22.5°$ and the absence of sharp peaks in the XRD patterns (Online

Resource 1, Fig. S2) confirmed the amorphous nature of the silica catalyst supports [30].

FESEM (Fig. 4) and TEM (Fig. 5) micrographs illustrated that the primary particles of the CFA-derived silica catalyst supports were approximately spherical with sizes ≤ 200 nm and had coalesced to form micron-size agglomerates in all samples. Surfactants are known to play a crucial role during silica nanoparticle synthesis from pure chemicals such as tetraethoxysilane (TEOS), influencing mesostructure formation, reducing particle diameters, and improving dispersion of the particles, thereby minimizing aggregation [31]. In the present work, elevated levels of aggregation were observed when SLS and PEG were used as surfactants whereas the use of CTAB and CPC hindered the aggregation of silica
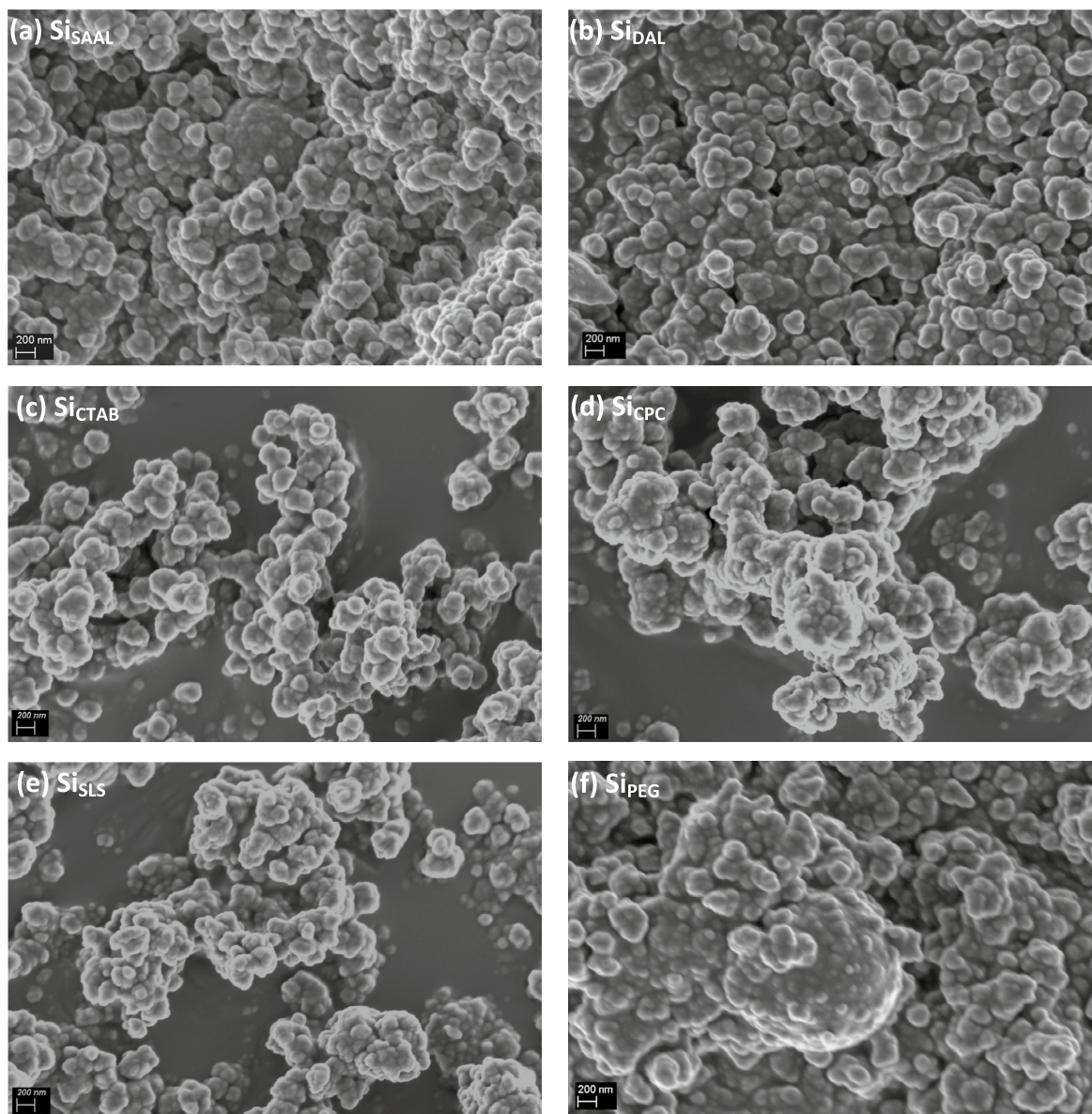

Fig. 4 FESEM images of the silica catalyst supports: **a** Si_{SAAL}, **b** Si_{DAL}, **c** Si_{CTAB}, **d** Si_{CPC}, **e** Si_{SLS} and **f** Si_{PEG}
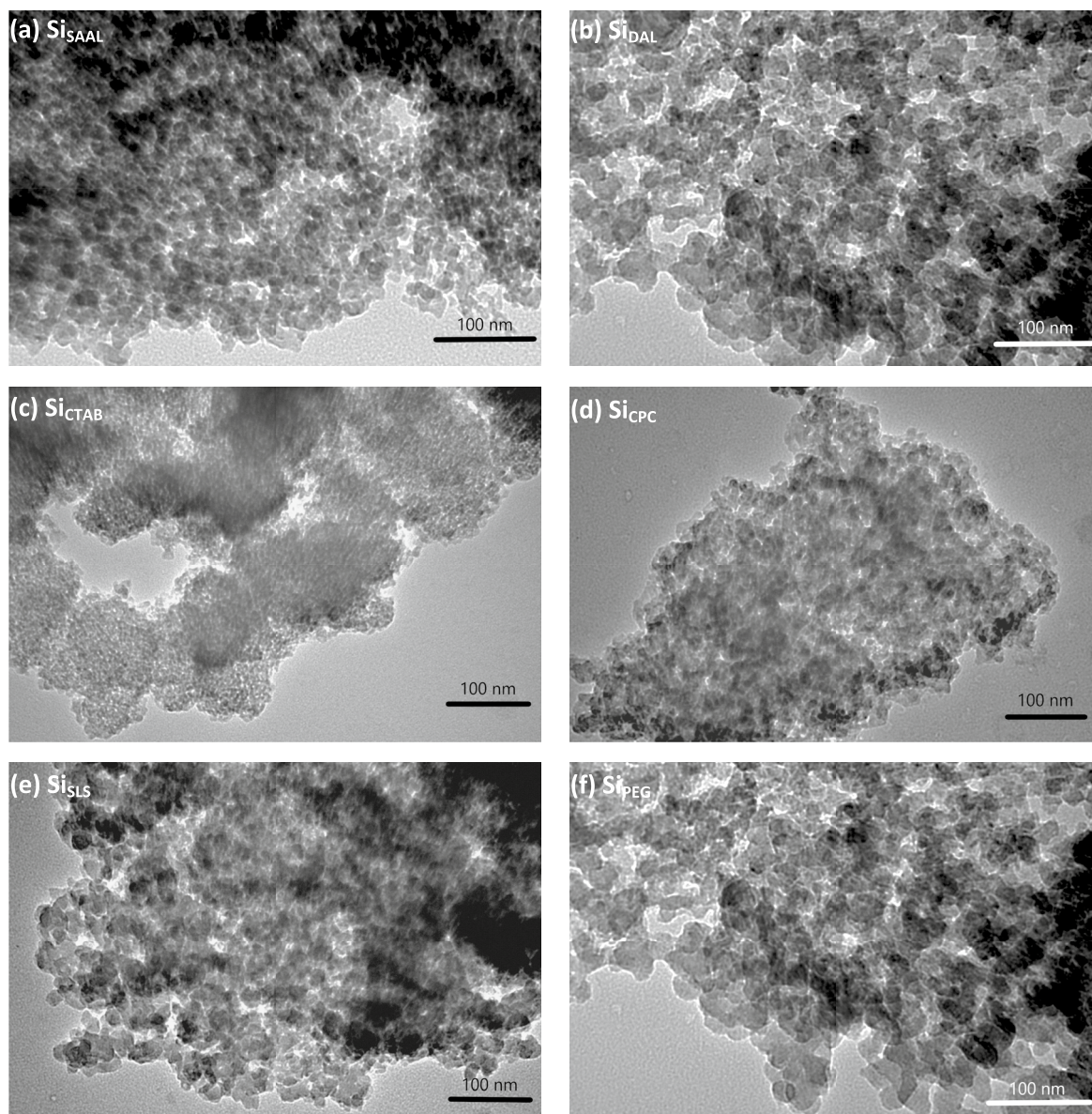
Fig. 5 TEM images of the silica catalyst supports: **a** Si_{SAAL}, **b** Si_{DAL}, **c** Si_{CTAB}, **d** Si_{CPC}, **e** Si_{SLS} and **f** Si_{PEG}

nanoparticles and enhanced their dispersion. Improved particle–particle separation has been reported in the literature when CTAB and dodecyl trimethylammonium bromide (DTAB) were used as surfactants during the synthesis of amorphous silica nanoparticles from a pure commercially available sodium silicate solution [30].

Textural properties (Table 1 and Online Resource 1, Fig. S3) of the CFA-derived silica catalyst supports indicated BET surface areas between 480 and 780 $m^2\,g^{-1}$, average pore diameters between 2.5 and 6.1 nm and pore volumes around 0.4 $cm^3\,g^{-1}$. According to IUPAC classification, the prepared silica catalyst supports can be classified as mesoporous materials, for which pore size is typically in the range of 2–50 nm [32]. The BET surface areas of the

CFA-derived supports were similar to that reported for SBA-15 ($> 700\ m^2\,g^{-1}$) and lower than MCM-41 ($> 1000\ m^2\,g^{-1}$), used as catalyst supports used in our previous studies [22, 23, 33].

The specific surface area and the porosity of the silica catalyst supports were greatly affected by the surfactant used during its synthesis. Figure 6 compares variation in surfactant chain length with the textural properties of the respective silica catalyst supports. CTAB and CPC are surfactants with 16-carbon chains, while SLS contains a 12-carbon chain (Online Resource 1, Fig. S4). The performance of PEG as a dispersant is discussed separately in the next paragraph and is therefore not included in the comparison between the effects of CTAB, CPC and SLS because the

Table 1 Textural properties of the silica catalyst supports and immobilized catalysts

	Silica catalyst supports			Immobilized catalysts		
	BET surface area $(m^2\ g^{-1})$	Average pore diameter (nm)	Pore volume $(cm^3\ g^{-1})$	BET surface area $(m^2\ g^{-1})$	Average pore diameter (nm)	Pore volume $(cm^3\ g^{-1})$
SAAL	515	2.74	0.35	426	8.23	0.87
DAL	651	2.52	0.41	415	6.45	0.70
CTAB	785	3.35	0.40	609	5.01	0.35
CPC	741	4.92	0.40	585	5.00	0.30
SLS	487	6.12	0.32	405	6.41	0.28
PEG	515	2.74	0.35	383	4.83	0.20

Fig. 6 Variation of the surfactant chain lengths vs textural properties of the silica catalyst supports
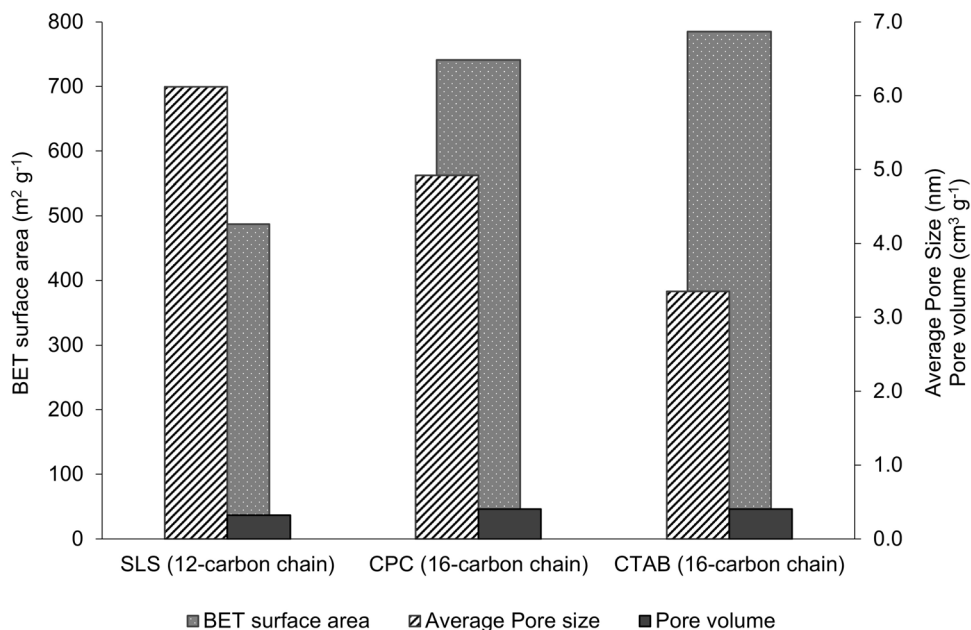
carbon chain structure of PEG is different from that of the other surfactants used.

Comparison between CTAB, CPC and SLS—A maximum specific surface area of 785 $m^2\ g^{-1}$ was obtained when using CTAB as surfactant. As the carbon chain length of the surfactant increased from SLS to CPC and CTAB (Fig. 6), the surface area of the silica catalyst supports increased from 487 $m^2\ g^{-1}$ for Si_{SLS} to 741 $m^2\ g^{-1}$ for Si_{CPC} and 785 $m^2\ g^{-1}$ for Si_{CTAB}. The cumulative pore volume increased from 0.32 $cm^3\ g^{-1}$ for Si_{SLS} to 0.40 $cm^3\ g^{-1}$ for both Si_{CPC} and Si_{CTAB} (Table 1). A decrease in the average pore size from 6.12 nm for Si_{SLS} (shortest chain length) to 3.35 nm for Si_{CTAB} and 4.92 nm for Si_{CPC} (longest chain length) with an increase in the carbon chain length was observed. Similar results have been reported in literature, i.e. that the pore size of silica nanoparticles can be reduced by increasing the chain length of the surfactant employed during its synthesis [30, 34]. Application of CTAB and CPC as dispersants during silica catalyst support synthesis resulted in an increase

in the pore volume of the nanoparticles and a substantial improvement in the BET specific surface area, with an increase of nearly two orders of magnitude (741–785 $m^2\ g^{-1}$; Table 1, Fig. 6) in comparison to the results achieved using SLS (486 $m^2\ g^{-1}$).

PEG—The textural properties of the silica catalyst supports prepared using PEG as surfactant were similar regardless of the composition of the Na_2SiO_3 solution used as precursor (Si_{SAAL} *vs* Si_{DAL}) or storage conditions (S_{SAAL} *vs* Si_{PEG}) (Table 1). The FESEM micrographs of these catalyst supports revealed dense aggregates consisting of closely packed particles, with only a few dispersed particles (Fig. 4a, b and f). The influence of PEG surface coverage on the physical properties of silica nanoparticles has previously been reported by Gao et al. [35]. These authors established that the particle size and size distribution of the obtained silica nanoparticles depend on the concentration of the PEG dispersion. At relatively low concentration, the amount of PEG was found to be insufficient to inhibit further growth of the

silica nanoparticles, leading to the formation of large aggregates of silica particles. An increase in PEG concentration led to an increase in the number of PEG aggregates forming in the aqueous solution, resulting in the formation of silica nanoparticles inside the entangled PEG chains. Therefore, to determine the optimal conditions for producing high-quality silica nanoparticles with good dispersion and uniformity, it is crucial to investigate the influence of surfactant surface coverage. The latter was outside the scope of this study.

In summary, while the studied surfactants led to the formation of silica nanoparticles with comparable particle sizes (≤ 200 nm), altering the type of surfactant used during the synthesis of the silica catalyst supports had a discernible impact on both the textural properties and dispersion of the resulting products.

Characterisation of Immobilized Catalysts

Immobilization of functionalized Cu(II) complex onto the silica catalyst supports made use of the general reaction scheme presented in Fig. 2. This process consisted of facilitating the condensation of the surface silanol groups (Si–OH) of the catalyst support with the $Si(OEt)_3$ group of the siloxane-functionalized Cu(II) complex, resulting in the formation of a covalently bound catalyst precursor [23]. Immobilized catalysts obtained using the CFA-derived silica supports synthesised from the two different grades of Na_2SiO_3 (Si_{SAAL} and Si_{DAL}) were labelled Cu_{SAAL} and Cu_{DAL}, while those obtained by varying the type of surfactant during its synthesis (Si_{CTAB}, Si_{CPC}, Si_{SLS} and Si_{PEG}) were labelled Cu_{CTAB}, Cu_{CPC}, Cu_{SLS} and Cu_{PEG}, respectively.

The XRD patterns of the CFA-derived immobilized catalysts were similar to those of their respective native supports (Online Resource 1, Fig. S2), indicating that the support materials had retained their amorphicity following the immobilization process.

The textural properties of the immobilized catalysts, calculated from BET analysis, are summarised in Table 1. The BET surface area of the immobilized catalysts decreased while the average pore diameter remained similar or showed a small increase when compared to that of the native supports. The decrease in the BET surface area can be ascribed to successful immobilization of the functionalized complex onto the silica catalyst support, leading to a decrease in the volume of nitrogen being absorbed due the immobilized complex occupying space on the surface of the catalyst support [23]. A general increase in the pore size was observed when the silica immobilized catalysts was compared to their respective native silica catalyst supports. A similar trend of decreasing surface area and increasing pore diameter in an SBA-15 immobilized catalyst was reported previously. This trend was attributed to the potential post-synthetic modification of the silica catalyst support during the immobilization

process, which was also carried out in toluene at 110 °C [23]. A substantial decrease in BET surface area and an increase in pore sizes were also reported for SBA-15 which was calcined at 540 °C and then hydrothermally treated in water at 100 °C [35]. According to our knowledge, there is no literature available regarding the influence of thermal treatment of mesoporous silica in toluene. This aspect is beyond the scope of the current study but will be addressed in our future work.

The pore volumes of Cu_{CTAB}, Cu_{CPC}, Cu_{SLS} and Cu_{PEG} were slightly smaller than those of their respective native supports. This would be expected when the complex is successfully tethered to the surface of the catalyst support thus resulting in a decrease in the pore volume. A similar observation was made by Malumbazo et al. during immobilization of a Cu(II) salicylaldimine complex onto a Davisil 710 silica support, tested as catalyst for cyclohexene oxidation [22]. In contrast, the pore volumes of Cu_{SAAL} and Cu_{DAL} were higher than that of their native catalyst supports. These results resemble the results reported before for immobilization of Cu(II) complexes on MCM-41 and SBA-15 silica supports [22, 23]. It is possible that in the case of the Si_{CTAB}, Si_{CPC}, Si_{SLS} and Si_{PEG} supports, the active sites for Cu(II) complex attachment were exposed on the surface of the silica supports leading to a decrease in pore volume, which was not the case for Si_{SAAL} and Si_{DAL} supports due to a lower concentration of surface hydroxyls (–OH). The active sites refer to the interaction or attachment of the Cu(II) complex to the surface or on the pores of the silica support. Another possibility could be differences in surface polarity of the different supports. The high surface polarity of silica, resulting from the high concentration of surface hydroxyls (–OH), will lead to facile catalyst attachment [22].

In this study, all CFA-derived catalyst supports were calcined at 650 °C to remove the excess surfactant. Amorphous silica nanoparticles are hygroscopic in nature and will readily absorb water molecules from the atmosphere. The influence of different storage conditions on the performance of the silica catalyst supports was examined to compare their performance as catalyst supports in the oxidation of veratryl alcohol to that of previously employed silica supports (MCM-41 and SBA-15). Si_{SAAL} and Si_{DAL} were stored under dry conditions to avoid absorption of water from the atmosphere. Meanwhile, Si_{CTAB}, Si_{CPC}, Si_{SLS} and Si_{PEG} were left to absorb moisture prior to immobilization of the metal complexes. Si_{SAAL} and Si_{PEG} were prepared using the same Na_2SiO_3 solution as a precursor and PEG as surfactant. Therefore, the only difference in the preparation of these two catalyst supports was their storage conditions.

Since Si_{SAAL} and Si_{DAL} were not exposed to moisture during storage, it was expected that these products will contain a lower concentration of surface hydroxyls (or silanol groups) compared to the other catalyst supports (Si_{CTAB},

Si$_{CPC}$, Si$_{SLS}$ and Si$_{PEG}$). The Si$_{CTAB}$, Si$_{CPC}$, Si$_{SLS}$ and Si$_{PEG}$ supports were expected to contain a high concentration of surface hydroxyls, leading to improved attachment of catalysts to the surface of these supports, compared to the Si$_{SAAL}$ and Si$_{DAL}$ supports which were expected to contain less surface hydroxyl groups. An adequate concentration of surface hydroxyls on the surface of the catalyst support is crucial. This is because catalyst attachment occurs through a condensation reaction between the surface silanol groups (Si–OH) on the silica catalyst support and the Si(OEt)$_3$ groups of the siloxane-functionalized Cu(II) complex, resulting in the formation of a covalently bound catalyst precursor (Fig. 2). Malumbazo et al. [22] reported the application of silica immobilized salicylaldimine Cu(II) complexes as catalysts in cyclohexene oxidation using three different types of silica supports, Davisil 710, MCM-41 and SBA-15. The Davisil 710 support was left uncalcined while both the MCM-41 and SBA-15 supports were calcined prior to immobilization of the metal complexes. Calcination of the silica supports reduced the number of silanol groups on the surface of the material, leading to a lower amount of the metal complex being anchored on the silica support. The presence of a high concentration of hydroxyl groups on the surface of uncalcined Davisil 710 facilitated catalyst attachment.

Process 1 (Fig. 1) was the preferred method for synthesizing the silica supports (Si$_{CTAB}$, Si$_{CPC}$, Si$_{SLS}$ and Si$_{PEG}$) because it produced silica nanoparticles of higher purity. However, when comparing the properties of Si$_{SAAL}$ *vs* Si$_{DAL}$ and Cu$_{SAAL}$ *vs* Cu$_{DAL}$ there is no direct evidence that the purity of the Na$_2$SiO$_3$ solution affected the properties of the synthesized coal fly ash derived silica catalyst supports or their associated immobilized catalysts.

FESEM and TEM micrographs of the CFA-derived immobilized catalysts indicated that the shape of the silica catalyst supports was retained after immobilization of the Cu(II) complex and that no significant changes occurred in the microstructure of the immobilized catalysts when compared to the data recorded for their respective native supports (Online Resource 1, Fig. S5 and Fig. S6). The presence of fine particles on the surface of the support materials was evident in the TEM images of all the immobilized catalysts (Online Resource 1, Fig. S6). These results are in agreement with results obtained for similar silica-supported catalyst systems [22, 23].

Catalytic Activity of Immobilized Catalysts During Oxidation of Veratryl Alcohol

Following characterization, the immobilized catalysts were evaluated as catalyst precursors in the oxidation of veratryl alcohol, using *tert*-butyl hydrogen peroxide (TBHP) as oxidant. TBHP has been successfully applied as oxidant for the oxidation of veratryl alcohol in various

catalytic systems, with varying yields of veratrylaldehyde and veratric acid being reported depending on the reaction conditions and catalyst employed [1, 8].

The reaction parameters were initially optimized employing the Cu(II) complex as homogenous catalyst in the oxidation of veratryl alcohol. A moderate conversion (68%) and good selectivity with yields of 85% veratrylaldehyde and 15% veratric acid were obtained. The optimized reaction conditions were found to be 2 mol % Cu loading, 1.0 mmol veratryl alcohol, 0.2 mmol NaOH and 2.0 mmol TBHP at 25 °C for 6 h using 10 ml acetonitrile as solvent.

After establishing reasonable activity in the homogeneous reaction mixture, the homogeneous system was heterogenized by immobilizing it onto silica supports MCM-41 and SBA-15, which were previously employed in similar catalytic systems. The resultant immobilized catalysts, Cu$_{MCM-41}$ and Cu$_{SBA-15}$ were evaluated as catalyst precursors in the oxidation of veratryl alcohol using the optimized reaction conditions employed for their homogeneous counterpart. The reaction scheme is given in Fig. 3. Reactions carried out using Cu$_{MCM-41}$ and Cu$_{SBA-15}$ immobilized catalysts exhibited low conversions (30–36%), with good selectivity towards the formation of veratrylaldehyde (80–90%), and small amounts of veratric acid (10–20%) being formed (Fig. 7 and Online Resource 1, Table S1).

The performance of the CFA derived catalysts was tested under the same catalytic conditions. All the CFA-derived immobilized catalysts were active in the oxidation of veratryl alcohol, with conversions ranging between 24 and 57% (Fig. 7 and and Online Resource 1, Table S1). Veratrylaldehyde and veratric acid were still found to be the main products. The results obtained for Cu$_{SAAL}$, and Cu$_{DAL}$ resembled that of immobilized catalysts Cu$_{MCM-41}$ and Cu$_{SBA-15}$. Low degrees of conversion (20–24%) and a high selectivity towards the formation of veratrylaldehyde (90–96%) were observed. This result suggests that overoxidation of veratrylaldehyde to veratric acid is restricted at low conversions, resulting in the formation of veratrylaldehyde as the primary product. The moderate activity of Cu$_{SAAL}$ and Cu$_{DAL}$ can most likely be attributed to poor catalyst immobilization onto these silica supports. This aspect will be discussed in further detail below. It was noticed that some physically adsorbed copper salt was leaching into the reaction mixture. The catalytic inactivity of the free copper salt was confirmed by testing Cu(OAc)$_2$H$_2$O as catalyst precursor in the oxidation of veratryl alcohol. Cu(OAc)$_2$H$_2$O, in absence of stabilization by an immobilized ligand, exhibited very low conversion (~8%) with predominantly veratrylaldehyde formation. This suggests that only copper coordinated via the immobilized ligand sites is active in this catalytic process, highlighting the necessity of ligand sites for stabilization of the active copper centres.

Fig. 7 Oxidation of veratryl alcohol with TBHP, heterogeneously catalyzed by a Cu(II) complex immobilized on MCM-41 (Cu$_{MCM-41}$), SBA-15 (Cu$_{SBA-15}$) and the CFA-derived catalyst supports (Cu$_{SAAL}$, Cu$_{DAL}$, Cu$_{CTAB}$, Cu$_{CPC}$, Cu$_{SLS}$ and Cu$_{PEG}$). Reaction conditions: veratryl alcohol (1 mmol), 2 mol % catalyst, temperature (25 °C), TBHP (2 mmol), acetonitrile (10 ml) and NaOH (0.2 mmol)
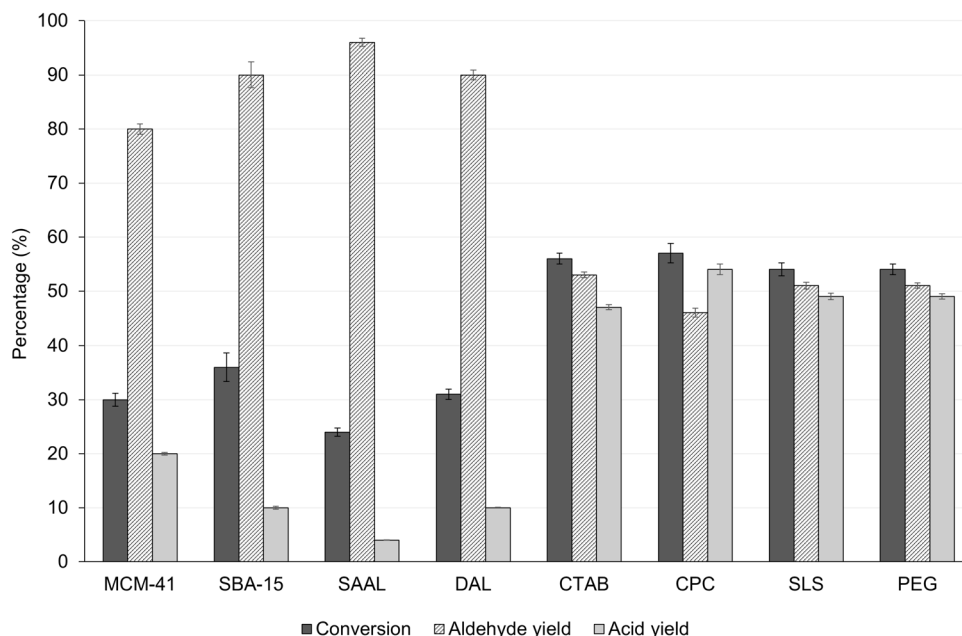
The use of immobilized catalysts Cu$_{CTAB}$, Cu$_{CPC}$, Cu$_{SLS}$ and Cu$_{PEG}$ improved the conversion of veratryl alcohol (50–52%). However, this resulted in the selectivity being compromised with product distributions of only approximately 50% veratrylaldehyde and veratric acid being observed. The higher catalytic activity achieved with these catalysts was likely attributed to their greater BET surface areas, as shown in Table 1. This increased surface area allowed for better access to the catalytically active sites, leading to higher activity but also resulting in overoxidation and the production of larger amounts of veratric acid [22, 36].

Si$_{SAAL}$ and Si$_{PEG}$ were prepared under the same experimental conditions but stored under different environmental conditions (Fig. 1). Storage of Si$_{PEG}$ under ambient conditions was expected to increase the concentration of surface silanol groups, resulting in more effective immobilization of the Cu(II) complex on the surface of Si$_{PEG}$ compared to Si$_{SAAL}$, evident by the low degree of conversion (20%) attained in the reaction system employing the Cu$_{SAAL}$ immobilized catalyst as compared to Cu$_{PEG}$ (50%). These observations confirmed the importance of having a sufficient amount of silanol groups on the surface of the silica catalyst support for successful catalyst attachment during immobilisation [37, 38].

These results clearly show that the nature of the catalyst support plays a significant role in the conversion rate and selectivity of the oxidation reaction tested. The presence of active catalytic sites on the surface of the catalyst will have a substantial effect on the selectivity of the catalyst. The difference in selectivity observed for immobilized catalysts Cu$_{CTAB}$, Cu$_{CPC}$, Cu$_{SLS}$ and Cu$_{PEG}$ might be attributed to the elevated concentration of surface hydroxyls in their native supports, enhancing catalyst immobilization and consequently extends the contact time between the substrate and the surface of the support. As a result, conversion of veratryl alcohol is increased. However, it may also lead to unintended overoxidation of veratrylaldehyde to veratric acid. The selectivity of immobilized catalyst Cu$_{SAAL}$ and Cu$_{DAL}$ towards the formation of veratrylaldehyde may subsequently be ascribed to the lower concentration of silanol groups available on the catalyst's surface [22].

Recyclability of the Catalysts

The durability and reusability of the CFA-derived immobilized catalysts were evaluated for the oxidation of veratryl alcohol with TBHP. The catalysts were recycled up to five times using the same reaction conditions, with the exception of Cu$_{SAAL}$ and Cu$_{DAL}$ which were only recycled three times due to loss of activity of these catalysts after three runs (Table 2). The continuous loss in activity for Cu$_{SAAL}$ and Cu$_{DAL}$ was attributed to an insufficient number of silanol groups on the surface of the support material, leading to a lower amount of the Cu(II) complex being anchored on the silica support. The selectivity towards formation of the veratrylaldehyde was retained.

Cu$_{CTAB}$, Cu$_{CPC}$, Cu$_{SLS}$ and Cu$_{PEG}$, displayed good recyclability over five catalytic runs. A slight decrease in activity was noted with conversions ranging from 42 to 57%. However, poor selectivity was observed with almost equal amounts of veratrylaldehyde to veratric acid being obtained. The slight drop-in activity was attributed to a loss of the catalyst during its recovery, as well as a low

Table 2 Recyclability and reusability of CFA-derived immobilized catalysts in the oxidation of veratryl alcohol with TBHP[a]

Cu$_{SAAL}$				Cu$_{DAL}$			
	Conversion (%)	Aldehyde yield (%)	Acid yield (%)		Conversion (%)	Aldehyde yield (%)	Acid yield (%)
Run 1	24	96	4		31	90	10
Run 2	19	95	5		24	83	17
Run 3	16	97	3		17	97	3
Cu$_{CTAB}$				**Cu$_{CPC}$**			
	Conversion (%)	Aldehyde yield (%)	Acid yield (%)		Conversion (%)	Aldehyde yield (%)	Acid yield (%)
Run 1	56	53	47		57	45	55
Run 2	51	48	52		56	53	47
Run 3	49	50	50		51	48	52
Run 4	51	45	55		49	50	50
Run 5	46	53	47		45	66	34
Cu$_{SLS}$				**Cu$_{PEG}$**			
	Conversion (%)	Aldehyde yield (%)	Acid yield (%)		Conversion (%)	Aldehyde yield (%)	Acid yield (%)
Run 1	54	51	49		54	51	49
Run 2	52	54	46		52	54	46
Run 3	54	48	52		54	48	52
Run 4	47	55	45		47	55	45
Run 5	42	60	40		45	58	42

[a]Reaction conditions: veratryl alcohol (1 mmol), 2 mol % catalyst, temperature (25 °C), TBHP (2 mmol), acetonitrile (10 ml) and NaOH (0.2 mmol)

degree of metal leaching into solution, which was visually detected by a slight green colour in solution. This reasoning is supported by the fact that slightly less of the veratrylaldehyde is being overoxidised to veratric acid after five catalytic runs.

These results thus show that Cu$_{CTAB}$, Cu$_{CPC}$, Cu$_{SLS}$ and Cu$_{PEG}$, can be utilized as a good recyclable heterogeneous catalyst in the oxidation of veratryl alcohol, with relatively low levels of metal leaching occurring during the catalytic reaction.

Impact of Oxidation Concentration

The impact of the concentration of the oxidant, TBHP was conducted. Changing the substrate to oxidant ratio from 1:2 to 1:3 resulted in almost a trembling of the conversion to around 70% (Fig. 8). Further increase in oxidant concentration showed very little enhancement of the conversion. However, the higher oxidant concentration had a significant impact on the selectivity of the reaction which at the higher TBHP levels showed a significant shift to the carboxylic acid product. It is clear that in the presence of higher levels of TBHP, oxidation of the intermediate aldehyde is facilitated, resulting in the carboxylic acid analogue being the predominant product.
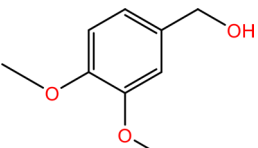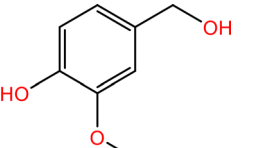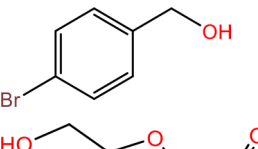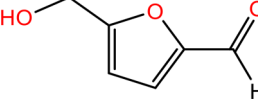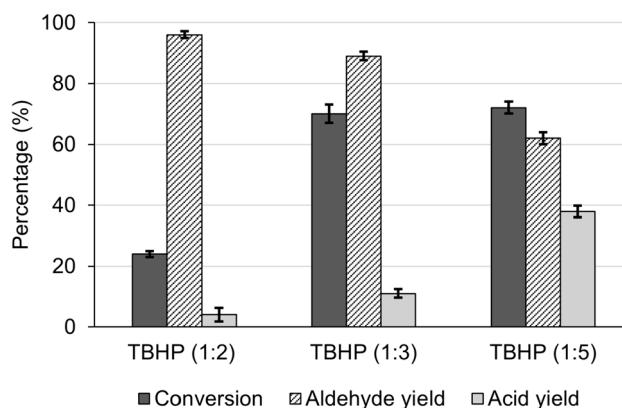

Fig. 8 Effect of TBHP concentration on activity using catalyst Cu$_{SAAL}$ in the oxidation of veratryl alcohol. Reaction conditions: veratryl alcohol (1 mmol), 2 mol % catalyst, temperature (25 °C), TBHP (2–5 mmol), acetonitrile (10 ml) and NaOH (0.2 mmol)

Substrate Scope

A preliminary investigation of the substrate scope of the catalytic system was carried out using two of the catalyst systems employed during the initial catalytic experiments, viz. Cu$_{SAAL}$ and Cu$_{CTAB}$. Thus, the reaction of veratryl alcohol (entry 1, Table 3) was compared with that of vanilyl alcohol (entry 2, Table 3). In addition, 4-bromo benzylalcohol (entry

Table 3 Evaluation of the substrate scope using Cu$_{SAAL}$ and Cu$_{CTAB}$ as catalysts

Entry	Substrate	Cu$_{SAAL}$			Cu$_{CTAB}$		
		Conversion (%)	Aldehyde yield (%)	Acid yield (%)	Conversion (%)	Aldehyde yield (%)	Acid yield (%)
1		70	91	9	84	41	59
2		72	89	11	80	45	55
3		67	82	18	75	43	57
4		62	79	21	83	40	60

Reaction conditions: alcohol (1 mmol), 2 mol % catalyst, temperature (25 °C), TBHP (3 mmol), acetonitrile (10 ml) and NaOH (0.2 mmol)

3, Table 3) as well as 5-(hydroxymethyl)furfural (entry 4, Table 3) were also employed substrates. The results indicate that both the Cu$_{SAAL}$ and Cu$_{CTAB}$ catalyst systems were able to effectively oxidise all of the alcoholic substrates in moderate to good yields. Once again, the Cu$_{CTAB}$ catalyst system was found to be slightly more active than the Cu$_{SAAL}$ catalyst system with having conversions around 80% and the latter having conversions between 60 and 70%. The Cu$_{CTAB}$ catalyst having the higher conversion also displays a higher selectivity to carboxylic analogue.

Conclusions

Application of mesoporous silica support materials such as SBA-15 and MCM-41 with uniform pore sizes, high surface areas, and large pore volumes are generally preferred as catalyst supports in heterogeneous catalysis. This study illustrates the suitability of CFA-derived amorphous mesoporous silica nanoparticles as catalyst support in heterogeneous catalysis. Our findings suggest that these products have the potential to serve as viable alternatives to commercially available mesoporous silica catalyst supports for the oxidation of veratryl alcohol, a lignin derived compound. The utilization of these catalyst systems could significantly contribute to the development of cost-effective and sustainable processes for producing value-added products from bio-derived substrates. The textural properties

of the CFA-derived silica catalyst supports were notably influenced by the surfactant used during its synthesis, while variation in storage conditions had an impact on the amount of silanol groups on the surface of the silica supports. The silanol groups are essential for the successful immobilisation of the catalyst. Pre-dealumination of CFA during Na$_2$SiO$_3$ preparation did not affect the performance of the catalyst supports. Preliminary investigation of the substrate scope revealed that both the catalyst systems, Cu$_{SAAL}$ and Cu$_{CTAB}$ were able to oxidise analogues of veratryl alcohol as well as the bio-renewable substrate 5-(hydroxymethyl)-2-furaldehyde. Further optimization is required to enhance both conversion and selectivity especially targeting the more valuable aldehyde products. Nevertheless, the results reported here are encouraging and lay the basis for the development of analogous "heterogenized" homogeneous catalysts using relatively cheap support material.

Data Availability The datasets generated during and/or analysed during the current study are not publicly available but are available from the corresponding author on reasonable request.

Declarations

Competing Interests The authors have no competing interests to declare.

References

1. Dhinagaran, G., Harichandran, G., Suvaitha, S.P., Venkatachalam, K.: Catalytic activity of SBA-15 supported CuO for selective oxidation of veratryl alcohol to veratraldehyde. Molecular Catalysis **528**, 112454 (2022). https://doi.org/10.1016/j.mcat.2022.112454

2. Habibi, D., Faraji, A.R.: Preparation, characterization and catalytic activity of a nano-Co(II)-catalyst as a high efficient heterogeneous catalyst for the selective oxidation of ethylbenzene, cyclohexene, and benzyl alcohol. C. R. Chim. **16**(10), 888–896 (2013). https://doi.org/10.1016/j.crci.2013.01.002

3. Lu, X., Hai, T., Gong, Z., Cao, Y., Wu, R., Yang, Y.: Heterogeneous catalyst for the veratryl alcohol oxidation based on gold nanoparticles decorated with graphene quantum dots supported on silicon dioxide. Results in Materials **6**, 100062 (2020). https://doi.org/10.1016/j.rinma.2020.100062

4. Tang, D., Zhang, W., Zhang, Y., Qiao, Z.A., Liu, Y., Huo, Q.: Transition metal complexes on mesoporous silica nanoparticles as highly efficient catalysts for epoxidation of styrene. J. Colloid Interface Sci. **356**(1), 262–266 (2011). https://doi.org/10.1016/j.jcis.2010.12.031

5. Unnarkat, A.P., Singh, S., Kalan, S.: Ethylbenzene oxidation using cobalt oxide supported over SBA-15 and KIT-6. Materials Today: Proceedings **45**, 3991–3996 (2021). https://doi.org/10.1016/j.matpr.2020.09.088

6. Yoganandhan, N., Tamizhdurai, P., Kavitha, C., Mangesh, V.L., Kumar, N.S., Al-Fatesh, A.S., Kumaran, R., Basivi, P.K.: TiO2/SO4/Ni@SBA-15 catalysts for the selective oxidation of veratryl alcohol to veratraldehyde in a continuous reactor. Molecular Catalysis **546**, 113250 (2023). https://doi.org/10.1016/j.mcat.2023.113250

7. Okolie, J.A., Nanda, S., Dalai, A.K., Kozinski, J.A.: Chemistry and specialty industrial applications of lignocellulosic biomass. Waste and Biomass Valorization **12**(5), 2145–2169 (2021). https://doi.org/10.1007/s12649-020-01123-0

8. Parida, N., Badamali, S.K.: Facile synthesis and catalytic activity of nanoporous SBA-1. J. Porous Mater. **29**(1), 161–167 (2021). https://doi.org/10.1007/s10934-021-01154-5

9. Fan, H., Yang, Y., Song, J., Ding, G., Wu, C., Yang, G., Han, B.: One-pot sequential oxidation and aldol-condensation reactions of veratryl alcohol catalyzed by the Ru@ZIF-8 + CuO/basic ionic liquid system. Green Chem. **16**(2), 600–604 (2014). https://doi.org/10.1039/c3gc41363b

10. Jana, N.C., Behera, S., Maharana, S.K., Behera, R.R., Bagh, B.: Selective aerobic oxidation of biomass model compound veratryl alcohol catalyzed by air-stable copper(ii) complexes in water. Catal. Sci. Technol.. Sci. Technol. **13**(18), 5422–5434 (2023). https://doi.org/10.1039/d3cy00671a

11. Melián-Rodríguez, M., Saravanamurugan, S., Kegnæs, S., Riisager, A.: Aerobic oxidation of veratryl alcohol to veratraldehyde with heterogeneous ruthenium catalysts. Top. Catal. Catal. **58**(14), 1036–1042 (2015). https://doi.org/10.1007/s11244-015-0472-z

12. Kervinen, K., Korpi, H., Leskelä, M., Repo, T.: Oxidation of veratryl alcohol by molecular oxygen in aqueous solution catalyzed by cobalt salen-type complexes: the effect of reaction conditions. J. Mol. Catal. A: Chem. **203**(1), 9–19 (2003). https://doi.org/10.1016/S1381-1169(03)00156-0

13. Mateo, C., Palomo, J.M., Fernandez-Lorente, G., Guisan, J.M., Fernandez-Lafuente, R.: Improvement of enzyme activity, stability and selectivity via immobilization techniques. Enzyme Microb. Technol.Microb. Technol. **40**(6), 1451–1463 (2007). https://doi.org/10.1016/j.enzmictec.2007.01.018

14. Zhang, Y., Ge, J., Liu, Z.: Enhanced activity of immobilized or chemically modified enzymes. ACS Catal.Catal. **5**(8), 4503–4513 (2015). https://doi.org/10.1021/acscatal.5b00996

15. Arzamendi, G., Campo, I., Arguiñarena, E., Sánchez, M., Montes, M., Gandía, L.M.: Synthesis of biodiesel with heterogeneous NaOH/alumina catalysts: comparison with homogeneous NaOH. Chem. Eng. J. **134**(1–3), 123–130 (2007). https://doi.org/10.1016/j.cej.2007.03.049

16. Singh, A.K., Yadav, R., Sakthivel, A.: Synthesis, characterization, and catalytic application of mesoporous SAPO-34 (MESO-SAPO-34) molecular sieves. Microporous Mesoporous Mater. **181**, 166–174 (2013). https://doi.org/10.1016/j.micromeso.2013.07.031

17. Zhang, Z., Pinnavaia, T.J.: Mesostructured γ-Al$_2$O$_3$ with a lath-like framework morphology. J. Am. Chem. Soc. **124**(41), 12294–12301 (2002). https://doi.org/10.1021/ja0208299

18. Kresge, C.T., Leonowicz, M.E., Roth, W.J., Vartuli, J.C., Beckt, J.S.: Ordered mesoporous molecular sieves synthesized by a liquid crystal template mechanism. Nature **359**, 710–712 (1992). https://doi.org/10.1038/359710a0

19. Zhao, D., Huo, Q., Feng, J., Chmelka, B.F., Stucky, G.D.: Nonionic triblock and star diblock copolymer and oligomeric surfactant syntheses of highly ordered, hydrothermally stable, mesoporous silica structures. J. Am. Chem. Soc. **120**(24), 6024–6036 (1998). https://doi.org/10.1021/ja974025i

20. Schmidt-Winkel, P., Lukens, W.W., Yang, P., Margolese, D.I., Lettow, J.S., Ying, J.Y., Stucky, G.D.: Microemulsion templating of siliceous mesostructured cellular foams with well-defined ultralarge mesopores. Chem. Mater. **12**(3), 686–696 (2000). https://doi.org/10.1021/cm991097v

21. Jana, S., Dutta, B., Bera, R., Koner, S.: Anchoring of copper complex in MCM-41 matrix: a highly efficient catalyst for epoxidation

of olefins by tert-BuOOH. Langmuir **23**(23), 2492–2496 (2007). https://doi.org/10.1021/la062409t

22. Malumbazo, N., Mapolie, S.F.: Silica immobilized salicylaldimine Cu(II) and Co(II) complexes as catalysts in cyclohexene oxidation: a comparative study of support effects. J. Mol. Catal. A: Chem. **312**(1–2), 70–77 (2009). https://doi.org/10.1016/j.molcata.2009.07.006

23. Kotzé, H., Mapolie, S.: Cationic ruthenium(II) complexes supported on mesoporous silica as catalyst precursors in the selective oxidative cleavage of 1-octene. Appl. Organomet. Chem.Organomet. Chem. **31**(7), e3643 (2017). https://doi.org/10.1002/aoc.3643

24. Reynolds-Clausen, K., Singh, N.: South africa's power producer's revised coal ash strategy and implementation progress. Coal Combustion and Gasification Products **11**, 10–17 (2019). https://doi.org/10.4177/CCGP-D-18-00015.1

25. Aphane, M.E., Doucet, F.J., Kruger, R.A., Petrik, L., Van Der Merwe, E.M.: Preparation of sodium silicate solutions and silica nanoparticles from south african coal fly ash. Waste and Biomass Valorization **11**(8), 4403–4417 (2020). https://doi.org/10.1007/s12649-019-00726-6

26. Cai, Q., Lin, W.-Y., Xiao, F.-S., Pang, W.-Q., Chen, X.-H., Zou, B.-S.: The preparation of highly ordered MCM-41 with extremely low surfactant concentration. Microporous Mesoporous Mater. **32**(1–2), 1–15 (1999). https://doi.org/10.1016/s1387-1811(99)00082-7

27. Mapolie, S.F., van Wyk, J.L.: Synthesis and characterization of dendritic salicylaldimine complexes of copper and cobalt and their use as catalyst precursors in the aerobic hydroxylation of phenol. Inorg. Chim. Acta. Chim. Acta **394**, 649–655 (2013). https://doi.org/10.1016/j.ica.2012.09.006

28. van Wyk, J.L., Mapolie, S.F., Lennartson, A., Håkansson, M., Jagner, S.: The catalytic oxidation of phenol in aqueous media using cobalt(II) complexes derived from N-(aryl) salicylaldimines. Inorg. Chim. Acta. Chim. Acta **361**(7), 2094–2100 (2008). https://doi.org/10.1016/j.ica.2007.10.031

29. van der Merwe, E.M., Prinsloo, L.C., Mathebula, C.L., Swart, H.C., Coetsee, E., Doucet, F.J.: Surface and bulk characterization of an ultrafine south african coal fly ash with reference to polymer applications. Appl. Surf. Sci. **317**, 73–83 (2014). https://doi.org/10.1016/j.apsusc.2014.08.080

30. Abou Rida, M., Harb, F.: Synthesis and characterization of amorphous silica nanoparitcles from aqueous silicates uisng cationic surfactants. Journal of Metals, Materials and Minerals **24**(1), 37–42 (2014). https://doi.org/10.14456/jmmm.2014.7

31. Yamada, H., Urata, C., Higashitamori, S., Aoyama, Y., Yamauchi, Y., Kuroda, K.: Critical roles of cationic surfactants in the preparation of colloidal mesostructured silica nanoparticles: control of mesostructure, particle size, and dispersion. ACS Appl. Mater. Interfaces **6**(5), 3491–3500 (2014). https://doi.org/10.1021/am405633r

32. Thommes, M., Kaneko, K., Neimark, A.V., Olivier, J.P., Rodriguez-Reinoso, F., Rouquerol, J., Sing, K.S.W.: Physisorption of gases, with special reference to the evaluation of surface area and pore size distribution (IUPAC technical report). Pure Appl. Chem. **87**(9–10), 1051–1069 (2015). https://doi.org/10.1515/pac-2014-1117

33. Leckie, L., Mapolie, S.F.: Mesoporous silica as phase transfer agent in the biphasic oxidative cleavage of alkenes using triazole complexes of ruthenium as catalyst precursors. Appl. Catal. ACatal. A **565**, 76–86 (2018). https://doi.org/10.1016/j.apcata.2018.07.038

34. Singh, L.P., Bhattacharyya, S.K., Mishra, G., Ahalawat, S.: Functional role of cationic surfactant to control the nano size of silica powder. Appl. Nanosci.Nanosci. **1**(3), 117–122 (2011). https://doi.org/10.1007/s13204-011-0016-1

35. Gao, G.-M., Zou, H.-F., Liu, D.-R., Miao, L.-N., Ji, G.-J., Gan, S.-C.: Influence of surfactant surface coverage and aging time on physical properties of silica nanoparticles. Colloids Surf. A **350**(1–3), 33–37 (2009). https://doi.org/10.1016/j.colsurfa.2009.08.030

36. Jha, A., Chandole, T., Pandya, R., Roh, H.-S., Rode, C.V.: Solvothermal synthesis of mesoporous manganese oxide with enhanced catalytic activity for veratryl alcohol oxidation. RSC Adv. **4**(37), 19450–19455 (2014). https://doi.org/10.1039/c4ra00184b

37. Jesionowski, T., Krysztafkiewicz, A.: Preparation of the hydrophilic/hydrophobic silica particles. Colloids Surf. A **207**, 49–58 (2002). https://doi.org/10.1016/S0927-7757(02)00137-1

38. Jesionowski, T., Krysztafkiewicz, A.: Infuence of silane coupling agents on surface properties of precipitated silicas. Appl. Surf. Sci. **172**, 18–32 (2001). https://doi.org/10.1016/S0169-4332(00)00828-X